Appl Phys A
DOI 10.1007/s00339-013-7846-5

Applied Physics A
Materials Science & Processing

RAPID COMMUNICATION

Alkali-treated Si nanowire array for improving solar cell performance

Yurong Jiang · Ruiping Qing · Haigang Yang · Chen Chen · Heng Ma · Fanggao Chang

Received: 24 March 2013 / Accepted: 4 July 2013

Abstract The Si nanowire array (SiNWA) was achieved by metal-assisted etching. The effect of alkali-treating of SiNWA on the photovoltaic performance of solar cells was investigated. We found that the post-chemical treatment of SiNWA on solar cells could reduce (i) the surface reflection and (ii) the thickness of "dead layer" so that the short-wavelength spectral response is enhanced. As a result, a solar-spectrum-averaged reflectance of less than 3 % has been reached, a 3-fold enhancement on the spectral response of post-treated SiNWA cell at the wavelength of 400 nm has been observed, together resulting in a remarkable improvement of 45 % in the conversion efficiency.

1 Introduction

Considerable interest exists for nanowire-based solar cells [1–3] due to their unique optical properties compared to bulk silicon and their potential to achieve high energy conversion efficiency at low cost [4, 5]. Therefore, Si nanowire (SiNW) structures are promising in the development of next-generation Si solar cells that suffer from insufficient light absorption for low-energy photons [6]. Despite the significant benefits from the one-dimensional Si nanostructure, the energy conversion efficiencies of SiNW solar cells are typically lower than those of their conventional Si counterparts, mainly due to their high surface recombination loss [7, 8]. In general, conventional SiNW solar cells that form a planar bulk junction inside the wafer exhibit poor spectral responses, especially in the short-wavelength region [9]. This feature is normally ascribed to the presence of a heavily doped thick emitter that acts as an electrically "dead layer" with high Auger recombination loss [10]. Absorption of short-wavelength photons in the high recombination Si nano-surface causes poor blue response that limits the short-circuit current density (J_{sc}). This near-surface recombination also reduces the open circuit voltage (V_{oc}) of the cell [11]. Strategies for reducing near-surface recombination while avoiding serious deterioration in solar cell performance are of significant importance for developing highly efficient SiNW solar cells [12]. Therefore, near-complete light absorptance throughout the whole solar spectrum is one of the vital factors for the development of next generation Si solar cells with high energy conversion efficiency and low production cost. Tapering the NWs by post-alkali dipping achieved separation of each NW from the bunched NWs, resulting in a strong enhancement of broadband optical absorption [13]. To our best knowledge, no one seams to have realized the importance of alkali treatment of SiNWs on the planar component to reduce the "dead layer" thickness and to improve the blue response of Si nanowire solar cell.

Here, we report an efficient approach for improving the spectral response and enhancing the surface antireflection. Simple chemical treatments were performed to optimize the solar cell performance. The alkali post-treatment removes the "dead layer" from SiNWA, which enables alleviating Auger recombination while separating the nanowires from the bundle. A much reduced light reflectance of less than 3 % has been achieved for the post-treated Si nanowire, thus improving the light harvesting of the solar cell. A remarkable enhancement (3-fold) in EQE near 400 nm revealed

Y. Jiang (✉) · R. Qing · H. Yang · C. Chen · H. Ma · F. Chang
College of Physics & Electrics Engineering, Henan Key Laboratory of Photovoltaic Materials, Henan Normal University, Xinxiang 453007, China
e-mail: jiangyurong@whut.edu.cn

F. Chang (✉)
e-mail: chfg@henannu.edu.cn

Published online: 26 July 2013

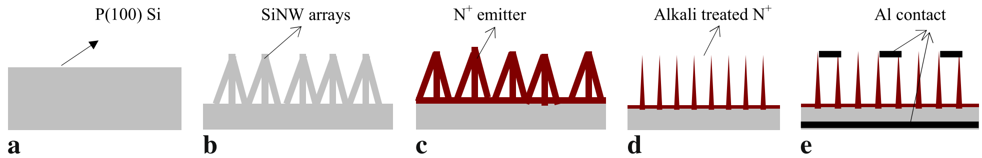

Fig. 1 Schematic illustration of the fabrication process for SiNWA -based solar cells: (**a**) initial p-type silicon wafer; (**b**) formation of bundled SiNWA on the wafer; (**c**) formation of n-type emitter by phosphorus diffusion; (**d**) alkali post-treated n-type emitter; (**e**) formation of electrodes on the rear and front surfaces

that reducing the "dead layer" thickness via alkali solution post-treating the cell surface also enhanced the conversion efficiency. The alkali-treated solar cell exhibited considerable enhancement in EQE over broadband wavelengths due to combined effects of superior light trapping and reducing the "dead layer" thickness in high surface area.

2 Experiment

SiNWA were grown on a p-type, 0.1–1 Ω/cm, Si(100) wafer by metal-assisted electroless etching. First, chemically–mechanically polished CZ silicon wafers of 5 cm in diameter were used to form a vertically aligned SiNW array in a mixed solution of deionized water, HF (4.6 M) and $AgNO_3$ (0.02 M) at room temperature. The etching was carried out in a simple teflon vessel. Before etching, the wafers were sequentially cleaned to remove the surface contaminants using the standard cleaning process for semiconductors. The wafers were then rinsed thoroughly with de-ionized water followed by 1 % HF solution to remove the native oxide. The cleaned silicon wafers were then immersed in the etching solution for 30 min to grow SiNWA. The samples obtained after etching were found to be wrapped with a thick Ag layer. Silver nanoparticles were easily removed using nitric acid after completion of the electroless etching. The samples were then rinsed with de-ionized water.

Two sets of SiNWA samples were prepared for cell fabrication: (i) samples with silicon nanowire array pre-treated in solution of 30 wt% NaOH for 30 s (at room temperature) before phosphorus doping and (ii) samples post-treated in the same conditions after phosphorus doping. Since the wet etching rate depends heavily upon the bond strengths of the surface atoms, the (111) planes exhibit the slowest etching rate, the surface planes of silicon wires were likely to develop in (111) planes during etching. Therefore, the etching rate of the tip was getting slower than that of the sidewalls consisting of (110) planes [14]. This results in a faster etching rate at the corner edges than at other flat regions. Thereby the sharp tips and tapered shape on the top-ends of the NWs were formed.

The n^+-emitter was formed by phosphorus diffusion using a $POCl_3$ liquid source at 880 °C for 10 min. Then phosphorous ions were doped via thermal diffusion into the surfaces of the wafer with NWA. The phosphosilicate glass that formed during $POCl_3$ diffusion was removed with 5 vol% HF. Finally, aluminum films of 600 nm thickness were deposited via thermal evaporation on the front and rear of the samples as grid electrodes and back contact, maintaining a light area of 0.5 cm^2. The schematic illustration of the cell fabrication process is shown in Fig. 1. In order to assess the effects of alkali post-treatment on the thickness of "dead layer" and consequently the cell performance, alkali pre-treated SiNWA cells were also prepared and studied as a comparison.

The as-synthesized SiNW arrays were characterized using a scanning electron microscope (SEM SUPRA™ 40). SiNW-based solar cells were cut out using the laser beam cutting machine. The reflectivity measurements were carried out by using a UV-3600 spectrophotometer with intergrating sphere working in the wavelength range of 300–2200 nm. The external quantum efficiency (EQE) spectra of the cells were characterized using a Newport 1000 W halogen lamp and a grating monochromator (Acton Spectra Pro 2300i) with an SR540 optical chopper and a lock-in amplifier (SR-830) to avoid the environmental electrical and optical interference. A calibrated Newport 818-UV sensor was employed for the absolute spectral responsibility EQE (in percents) evaluation of the solar cells. Solar cell performance was measured at AM 1.5 G illumination.

3 Results and discussion

Figure 2 presents tilted and cross-sectional scanning electron microscopic (SEM) images of the surfaces and cross-section of typical solar cells with SiNWA. Figure 2(a) reveals a bunched morphology between the top-ends of n-type emitters obtained by phosphorus diffusion in the as-etched NWs. It is well known that van der Waals force exists between the nano-structures with larger specific surface areas, resulting in silicon nanowire arrays bundled together, which is adverse to the absorption of sunlight. Figure 2(b) reveals a morphology in which the top-ends of alkali-treated NWs are separated. The agglomerated top-ends of the NW array could be easily separated from each other by even short time (30 s) treatment with NaOH during which the single

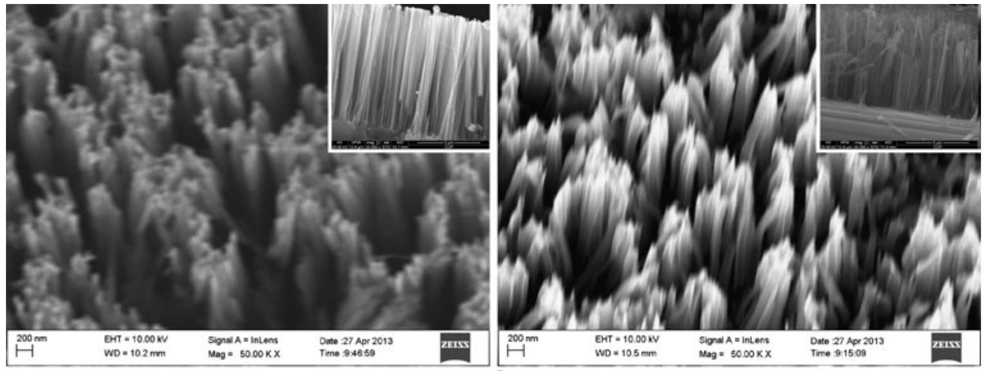

Fig. 2 Morphology of SiNWA solar cells. SiNWA were formed using metal-assisted etching: (**a**) plane-view SEM images of an untreated SiNWA solar cell; (**b**) plane-view SEM images of a SiNWA solar cell treated with alkali solution for 30 s after phosphorus diffusion. Insets: Cross-sectional SEM images (scale bars, 1 μm)

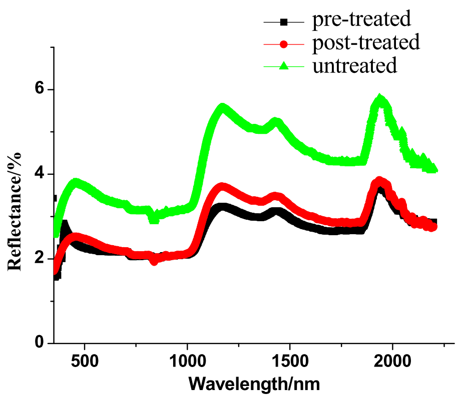

Fig. 3 Optical reflectance spectra of various SiNWA solar cells: untreated SiNWA (*triangles*), SiNWA alkali pre-treated for 30 s before (*squares*) and post-treated after (*circles*) phosphorus diffusion

nanowire etched into tapered nanowire by the alkali solution. The uniform distribution of the tapered nanowires is demonstrated in Fig. 2(b).

The antireflection behavior of SiNW layers was first evaluated. The total spectra light reflection on SiNWA solar cells that have undergone different alkali-treatment was measured using a UV-3600 spectrophotometer with an integrating sphere working in a wavelength range of 350–2200 nm. Figure 3 shows the reflectance spectra of SiNWA solar cells with and without alkali-treatment. The reflectance of the alkali pre-treated NWA and alkali post-treated NWA cells are all greatly decreased in the whole wavelength range compared to that of the untreated one. Superior antireflection characteristics with an average reflectance of less than 3 % are observed for both treated samples in wavelengths shorter than 1100 nm. This low reflectance for alkali-treated SiNWA can be ascribed to the ultrahigh surface area formed by tapering NWA. Incident light rays reflect between separate nanowires and would be almost entirely absorbed before they can leave the cell surface. These results show that the alkali-treatment can reduce the reflectivity of SiNWA significantly, and the uniform distribution of the nanowires is beneficial to the absorption of sunlight in a wide wavelength range. Therefore, alkali-treated SiNWA are promising in the development of the next-generation Si solar cells that suffer from insufficient light absorption.

The recombination losses are known to occur through two major routes, namely surface and Auger recombinations [10]. Since most high-energy photons are absorbed near the surface of wires, recombination loss is dramatic in a short-wavelength region. Based on our optical results, it is clear that alkali-treatment leads to a considerable improvement in optical response. To further highlight the effects of alkali treatment, the external quantum efficiency (EQE) of three typical samples: untreated NWA solar cell, alkali pre-treated before phosphorus diffusion, and alkali post-treated after phosphorus diffusion are shown in Fig. 4(a). Compared to the untreated and pre-treated NWA solar cells, the EQE of the post-treated sample is highest and reaches a peak value of 47.49 % at the wavelength of 690 nm. The EQE of untreated SiNWA solar cells is lowest and reaches its peak value of 44.25 % at the wavelength of 680 nm. Compared to the untreated sample, a remarkable ∼3-fold EQE enhancement at 400 nm wavelength is achieved for post-treated SiNWA solar cells (Fig. 4(b)). It can also be seen that the spectral response of the post-treated SiNWA cell is higher than that of the pre-treated cell within the visible light region from 400 to 750 nm, indicating that the post-treating SiNWA cell with alkali solution enhances the charge separating more effectively compared with pre-treating. In short, the short wavelength response for the post-treated device is significantly better than that for the pre-treated and untreated samples. Since the reflectance of both pre-treated and post-treated SiNWA cells is similar, the improvement of blue response for the post-treated sample implies that the low recombination loss might be responsible to the additional enhancement in conversion efficiency. It seems likely that the post-treatment of n-type emitter is capable of enhancing the charge separation by reducing the thickness of “dead layer”. Compared to the pre-treated solar cell, the EQE of post-treated cells shows that the blue response improves significantly, indicating that recombination within the electrically “dead layer” of untreated and pre-treated SiNWA evidently

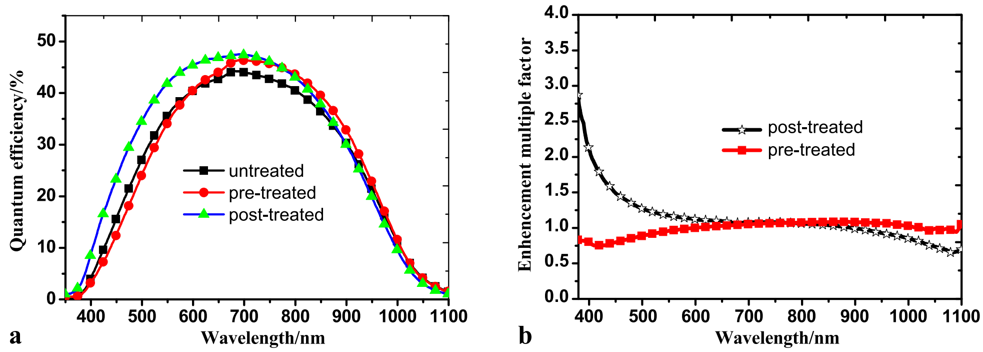

Fig. 4 (**a**) EQE of various SiNWA solar cells: untreated SiNWA (*black line*), alkali pre-treated SiNWA for 30 s before phosphorus diffusion (*red line*), alkali post-treated SiNWA for 30 s after phosphorus diffusion (*blue line*). (**b**) EQE enhancement factor of alkali-treated SiNWA solar cells: pre-treated (*black line*), post-treated (*red line*)

Table 1 The open circuit voltage (V_{oc}), short circuit current density (J_{sc}), filler factor (FF), Series resistance (R_s), bypass resistance (R_{sh}) and conversion efficiency of SiNWA Solar Cells

	V_{oc} (V)	J_{sc} (mA/cm^2)	FF (%)	R_s (Ω)	R_{sh} (Ω)	Convertion efficiency (%)
Pre-treated	0.385	15.42	38.5	20.84	189.75	2.29
Post-treated	0.3925	18.02	39.6	19.62	186.46	2.80
untreated	0.368	14.18	36.8	22.92	163.75	1.92

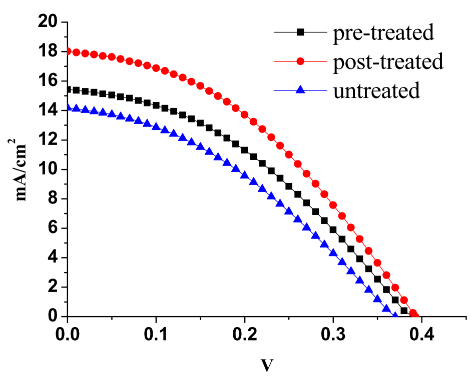

Fig. 5 *I–V* characteristics of various SiNWA solar cells: post-treated SiNWA (*red*); pre-treated SiNWA (*black*); untreated SiNWA (*blue*)

limits the blue EQE. Therefore, the main effect of alkali post-treatment is to improve the spectra response rather than reducing the reflectance.

Two factors may contribute to the nano-recombination layer with no photovoltaic response [10]: (i) surface recombination due to the large surface area of the nanoporous layer and (ii) Auger recombination arising from heavy emitter doping by heavy in-diffusion of phosphorus from the nanostructured surface area. The dead layer was attributed to high doping concentration in the nanoporous layer and additional recombination at the enormous internal surface [11]. According to the previous work, texturing emitter slightly using plasma immersion implantation can increase the minority lifetime and reduce the surface recombination rate [15]. Alkali post-treatment reduces the thickness of heavy doping emitter layer on the top of SiNWs and thus results in a thinner "dead layer" and increased the minority lifetime. As a result, the auger recombination problems would be alleviated and the blue response dramatically improved. Therefore, post-treated SiNWA cell represents a compromise between Auger recombination and surface recombination.

The effect of alkali-treatment on the performance of SiNWA solar cells was also examined by measuring the I–V characteristics under AM 1.5 G illumination (Fig. 5), and the result is summarized in Table 1. The short-circuit current density (J_{sc}) of the alkali post-treated solar cell is increased from 14.18 to 18.02 mA/cm^2, reflecting a 27 % enhancement compared to the untreated SiNW solar cell. The conversion efficiency of the alkali post-treated solar cell is increased from 1.92 % to 2.8 %, reflecting a 45 % enhancement compared to the untreated one. Measurements were repeated with different sets of samples and highest open circuit voltages (V_{oc}) and (J_{sc}) have been consistently obtained with the post-treated SiNWA solar cell. In general, the overall performance of SiNWA solar cells is improved by alkali-treatment. This is largely due to the J_{sc} enhancement, which stems from reducing the "dead layer" thickness and the surface recombination loss. This is also in good accordance with the EQE result that shows improved conversion efficiencies over the entire spectrum (Fig. 4).

The photovoltaic conversion efficiency is not as high as expected from the excellent antireflecting properties. We suggest that the low conversion efficiency may be a result of low current-collection efficiency of the front grid electrodes. To improve the main photovoltaic parameters such as short-circuit current and open-circuit voltage, some technological regimes including phosphorus diffusion and contacts fabrication should be optimized. Our work is now focusing on the improvement of these technological regimes.

4 Conclusions

An effective method for improving the conversion efficiency of Si NWA solar cells has been demonstrated. Alkali post-treatment has been applied to improve the light absorption and enhance solar cell performance by improving the blue spectral response. This result confirms that removing an electrically "dead layer" and reducing the surface recombination loss by post-treating the SiNWA lead to an efficiency enhancement of 45 %. This fact emphasizes the importance of surface treatment of SiNWs to obtain efficient SiNWs solar cells, and alkali post-treated SiNWA would be the preferred option. Although the nanowire-based photovoltaic cells still show a lower efficiency than those without nanowires under the present conditions, we believe that further improvements can be made that would eventually provide higher efficiencies.

Acknowledgements This work is supported by Chinese Nature Science Foundation Committee (No. 11074066) and Henan Provincial Basic and Frontier Project (No. 132300410248).

References

1. H. Fang, X. Li, S. Song, Y. Xu, J. Zhu, Nanotechnology **19**, 255703 (2008)
2. B. Ozdemir, M. Kulakci, R. Turan, H.E. Unalan, Nanotechnology **22**, 155606 (2011)
3. J.-Y. Jung, K. Zhou, J.H. Bangand, J.-H. Lee, J. Phys. Chem. C **116**, 12409 (2012)
4. J. Zhu, C.-M. Hsu, Z. Yu, S. Fan, Y. Cui, Nano Lett. **10**, 1979 (2010)
5. J. Zhu, Z. Yu, G.F. Burkhard, C.-M. Hsu, S.T. Connor, Y. Xu, Q. Wang, M. McGehee, S. Fan, Y. Cui, Nano Lett. **9**, 279 (2009)
6. E. Garnett, P. Yang, Nano Lett. **10**, 1082 (2010)
7. Y.P. Dan, K. Seo, K. Takei, J.H. Meza, A. Javey, K.B. Crozier, Nano Lett. **11**, 2527 (2011)
8. Y. Liu, T. Lai, H. Li, Y. Wang, Z. Mei, H. Liang, Z. Li, F. Zhang, W. Wang, A.Y. Kuznetsov, X. Du, Small **81**, 392 (2012)
9. K. Peng, Y. Xu, Y. Wu, Y. Yan, S.-T. Lee, J. Zhu, Small **1**, 1062 (2005)
10. F. Toor, H.M. Branz, M.R. Page, K.M. Jones, H.-C. Yuan, Appl. Phys. Lett. **99**, 103501 (2011)
11. H.-C. Yuan, V.E. Yost, M.R. Page, P. Stradins, D.L. Meier, H.M. Branz, Appl. Phys. Lett. **95**, 123501 (2009)
12. J. Oh, H.-C. Yuan, H.M. Branz, Nat. Nanotechnol. **7**, 743 (2012)
13. J.-Y. Jung, Z. Guo, S.-W. Jee, H.-D. Um, K.-T. Park, J.-H. Lee, Opt. Express **18**, A286 (2010)
14. X. Li, H.-S. Seo, H.-D. Um, S.-W. Jee, Y.W. Cho, B. Yoo, J.-H. Lee, Electrochim. Acta **54**, 6978 (2009)
15. Z. Shen, B. Liu, Y. Xia, J. Liu, J. Liu, S. Zhong, C. Li, Scr. Mater. **68**, 199 (2013)